Determination of Radiative Transition Widths of Excited States in C^{12}†

H. L. CRANNELL AND T. A. GRIFFY
High-Energy Physics Laboratory, Stanford University, Stanford, California
(Received 14 August 1964)

New absolute values for the elastic and inelastic electron-scattering cross sections from C^{12} are presented for a range of q^2 from 0.75 to 3.14 F^{-2}. A new method of analysis has been employed to obtain the radiative widths for the first three excited states in C^{12} from the measured inelastic cross sections. This method of analysis does not depend on a model for the transition charge distribution and is useful in determining the multipolarity of the transition.

INTRODUCTION

HIGH-ENERGY electron scattering has long been recognized as a powerful method for studying the electromagnetic structure of the atomic nucleus. In addition, as has been observed by Schiff,[1] inelastic electron-scattering resulting in the excitation of nuclear levels can be used to determine the multipolarities and lifetimes of the excited states. Previous experimenters have used the results of inelastic electron scattering to obtain the lifetimes for various nuclear levels.[2]

The nucleus C^{12} has been the subject of earlier investigations using high-energy electrons,[3] and the lifetimes of the two lowest excited states have been determined previously. It was pointed out by Salpeter,[4] that the lifetime of the 7.66-MeV level in C^{12} is of considerable importance in determining the rate of C^{12} production in certain stellar processes. Fowler,[5] and Seeger and Kavanaugh[6] have pointed out the need for a more accurate determination of the lifetime of this state at the present time. By using new and improved apparatus, and taking advantage of improvements in the Stanford Mark III linear accelerator, it has been possible to obtain new and more accurate cross sections for elastic and inelastic electron scattering from C^{12}. In addition, a method of obtaining the multipolarities and lifetimes of nuclear excited states that is independent of nuclear models has been developed. Lifetimes of the three lowest excited states in C^{12} have been determined.

EXPERIMENTAL PROCEDURE AND RESULTS

A thin carbon target (0.475 g cm^{-2}) was placed at the focus of a momentum-analyzed beam produced by the linear accelerator. With an incident electron energy of 250 MeV, elastic scattering and inelastic scattering resulting from the excitation of the 4.43-, 7.66-, and the 9.64-MeV levels in C^{12} were studied for each 5° step from 40 to 90°. Two measurements at 187-MeV and two at 300-MeV incident electron energy were made for comparison.

The scattered electrons were momentum-analyzed with the 72-in. 180° double-focusing spectrometer previously described by Hofstadter *et al.*[7] The electrons were detected with a 10-channel scintillation counter, also described in Ref. 7. The 10 scintillators were placed in a nonoverlapping pattern along the theoretical image plane of the spectrometer. For the range of spectrometer settings employed in this experiment, each scintillator had a fractional momentum acceptance of 0.34%. To reduce the background pulse rate, a coincidence was required between one of the scintillator detectors and a liquid-filled Čerenkov detector that was positioned immediately behind the 10-channel detector. The coin-

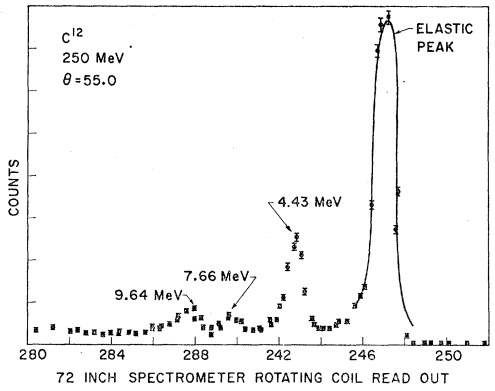

FIG. 1. Momentum spectrum of scattered electrons at 55° for an incident energy of 250 MeV. The abscissa gives values of the output of the rotating-coil magnetic-field monitor in the spectrometer. This output is adjusted so that it corresponds closely to the scattered electron momentum in units of MeV/c. The ordinate gives the number of counts arbitrarily normalized. The errors shown with each point are statistical only. Not shown is an uncertainty in the momentum position of each point due to the uncertainty in the exact position of the scintillators and in the dispersion of the spectrometer. These uncertainties amount to about 0.04% of the scattered momentum, or approximately 0.1 MeV/c in this case.

† This work was supported in part by the U. S. Office of Naval Research and the U. S. Air Force through the Air Force Office of Scientific Research. The computational work was supported by a grant from the National Science Foundation.

[1] L. I. Schiff, Phys. Rev. **96**, 765 (1954).

[2] W. C. Barber, Ann. Rev. Nucl. Sci. **12**, 1 (1962). This article contains a general review of inelastic electron scattering.

[3] J. H. Fregeau and R. Hofstadter, Phys. Rev. **99**, 1503 (1955); J. H. Fregeau, Ph.D. thesis, Stanford University, 1956 (unpublished).

[4] E. E. Salpeter, Phys. Rev. **107**, 516 (1957).

[5] W. Fowler (private communication).

[6] P. A. Seeger and R. W. Kavanaugh, Astrophys. J. **137**, 704 (1963).

[7] R. Hofstadter, F. A. Bumiller, B. R. Chambers, and M. Croissiaux, *Proceedings of the International Conference on Instrumentation for High-Energy Physics* (Interscience Publishers Inc., New York, 1960).

TABLE I. C^{12} cross sections for elastic and inelastic scattering of electrons.

E_0 (MeV)	θ	Elastic scattering (in 10^{-31} cm²/sr) $d\sigma/d\Omega$	Errors Area	Total	4.43-MeV level (in 10^{-31}cm²/sr) $d\sigma/d\Omega$	Errors Area	Total	7.66-MeV level (in 10^{-32} cm²/sr) $d\sigma/d\Omega$	Errors Area	Total	9.64-MeV level (in 10^{-32} cm²/sr) $d\sigma/d\Omega$	Errors Area	Total
187	84.0	3.76	0.05	0.12	1.86	0.03	0.06	2.96	0.15	0.17	5.83	0.58	0.61
	91.8	1.17	0.02	0.04	1.08	0.02	0.04	1.71	0.08	0.10	3.94	0.39	0.41
250	40.0	417.	5.	13.	26.6	1.0	1.2	63.1	3.9	4.3	59.3	7.4	7.6
	45.0	167.	2.	5.	16.4	0.4	0.7	42.2	1.7	2.1	47.4	2.8	3.1
	50.0	66.8	0.6	2.1	11.0	0.2	0.4	28.2	0.9	1.2	37.0	1.1	1.6
	55.0	27.0	0.3	0.9	7.01	0.14	0.25	15.8	0.8	0.9	26.2	0.9	1.2
	66.0	10.3	0.1	0.3	4.79	0.07	0.16	8.08	0.40	0.47	15.2	0.5	0.7
	65.0	4.04	0.05	0.13	3.26	0.05	0.11	4.65	0.23	0.27	11.0	0.4	0.5
	70.0	1.44	0.02	0.05	1.94	0.02	0.06	2.12	0.05	0.08	8.24	0.12	0.27
	75.0	0.420	0.008	0.016	1.28	0.01	0.04	1.30	0.04	0.06	5.57	0.08	0.18
	80.0	0.124	0.003	0.005	0.702	0.006	0.022	0.574	0.021	0.027	3.80	0.04	0.12
	85.0	0.0314	0.0010	0.0014	0.451	0.004	0.014	0.311	0.010	0.013	2.56	0.02	0.08
	90.0	0.0057	0.0003	0.0003	0.242	0.002	0.007	0.095	0.005	0.006	1.46	0.01	0.05
300	49.2	17.4	0.1	0.5	7.69	0.09	0.25	10.8	2.1	2.2	32.9	6.1	6.2
	54.8	4.30	0.04	0.14	4.12	0.05	0.13	4.90	0.49	0.51	19.5	2.0	2.0

cidence requirement reduced the background pulse rate to a negligible level.

At each scattering angle studied in this experiment the momentum spectrum of the scattered electrons showed peaks due to elastic scattering and due to the excitation of nuclear levels. One such spectrum is shown in Fig. 1. Eight or more momentum settings of the spectrometer were used to span the region of the spectrum under investigation. The momentum settings of the spectrometer were chosen so that each portion of the spectrum was observed several times. By maintaining the energy resolution of the incident beam at $\frac{1}{3}\%$ or better, the total resolution obtained in the scattered spectra was better than $\frac{1}{2}\%$.

The cross section for excitation of the 7.66-MeV level was much lower than the cross section for the elastic peak. In order to obtain comparable statistical accuracy in the cross sections for this level, more integrated beam current was used for those spectrometer settings during which the 10-channel counter spanned this level. With this technique, the relative uncertainties in the different cross sections were small. For all angles of 60° or less, at least 300 counts were obtained in each channel for all settings of the spectrometer.

Absolute values of the cross section associated with each peak were determined by comparison with electron scattering from protons in a polyethylene target. The absolute values of the proton cross sections were calculated using values of the form factors given by Hand *et al.*[8] and using some additional more recent determinations by Janssens.[9]

The data from each setting of the spectrometer were fed to an IBM-7090 computer. The computer was programmed to correct the data for differences in channel efficiencies, counting rates, spectrometer dispersion, and for different amounts of integrated beam current. The computer output was fed to a Calcomp plotter where the data were automatically plotted and labeled. Figure 1 is a reproduction of one of these plots.

The computer was also programmed to correct the measured spectrum for the effects due to bremsstrahlung and Schwinger radiation.[10] The resulting unfolded spectrum was then a theoretical representation of the shape of the spectrum in which no radiation processes were present. The unfolded spectrum was then automatically plotted in the same manner as the original spectrum. Figure 2 shows the results of unfolding the radiative effects from the spectrum shown in Fig. 1.

In order to minimize any uncertainties in the cross sections due to the radiative unfolding procedure, the data from the polyethylene target were analyzed in the same manner as the C^{12} data. It was encouraging to note that the estimates of the radiation correction given by the unfolding program were always within a few percent

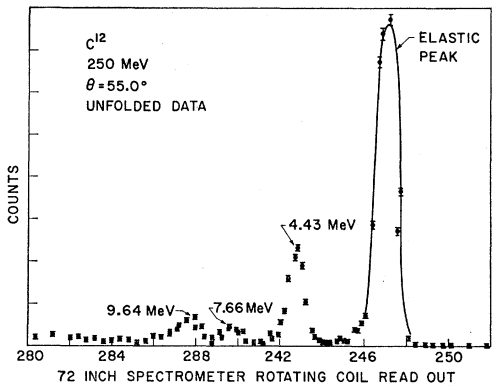

FIG. 2. Radiation-corrected momentum spectrum of scattered electrons at 55° for an incident energy of 250 MeV. This figure shows an experimental spectrum with the effects due to radiative losses of the electrons removed. The peaks in the corrected spectra are used to determine the cross sections.

[8] L. N. Hand, D. G. Miller, and Richard Wilson, Rev. Mod. Phys. **35**, 335 (1963).

[9] T. Janssens (private communication).

[10] H. Crannell (unpublished).

of the correction that would have been obtained using the more conventional method.[11]

The values of the measured elastic and inelastic cross sections for electron scattering from C^{12} are given in Table I. Two error assignments are given with each cross section. The errors given in the columns headed "Area" arise solely from the statistical error associated with determining the number of counts in the peak. The errors in the columns headed "Total" include in addition other uncertainties such as target density and thickness, and statistics associated with the measurement of the calibrating proton cross section. Errors due to uncertainties in the absolute proton cross section and errors in radiative unfolding are not included. The uncertainties in the measured proton cross sections are approximately 5%. For this experiment, uncertainty in the radiation corrections, which arise largely from approximations in the theoretical formulations of the radiative effects, are less than 5%.

ANALYSIS OF RESULTS

In this section, the analysis which was used to obtain the radiative widths $\Gamma_{E\lambda}$ from the measurement of the inelastic scattering cross section is presented. The Born approximation is assumed to be valid, i.e., the electron-nucleus interaction is described by the exchange of one virtual photon. Numerical calculations, including the Coulomb distortion of the electron wave function,[12] indicate that this assumption is quite good for light nuclei such as carbon in regions away from the diffraction minima in the cross section.

The differential cross section for inelastic electron scattering, exciting an electric multipole transition of order λ, may be written in the general form[2]

$$d\sigma/d\Omega=\sigma_{\mathrm{Mott}}\{F_{c\lambda}^2(q^2)+\tfrac{1}{2}[1+2\tan^2(\tfrac{1}{2}\theta)]F_{E\lambda}^2(q^2)\}. \quad (1)$$

The first term in Eq. (1) represents the longitudinal (Coulomb) part of the interaction, while the second term gives the contribution of the transverse part of the interaction. Measurements of the cross section at different angle θ (for the same value of q^2) made in this experiment seem to indicate that the second (transverse) term is not important in the cases considered here. In what follows the transverse part of the interaction is neglected and the cross section is written as

$$d\sigma/d\Omega=\sigma_{\mathrm{Mott}}F_\lambda^2(q^2). \quad (2)$$

The inelastic form factor $F_\lambda(q^2)$ is defined in terms of a reduced matrix element by the equation

$$F_\lambda(q^2)=[4\pi/(2J_i+1)]^{1/2}\langle f\|j_\lambda(qr)\|i\rangle, \quad (3)$$

where J_i is the ground-state spin of the target nucleus and the reduced matrix element is defined in terms of the matrix elements of the transition charge distribution $\rho_N(\mathbf{r})_{fi}$ by the equation[2]

$$\int j_\lambda(qr)Y_\lambda^\mu(\hat{r})\rho_N(\mathbf{r})_{fi}d^3\mathbf{r}$$

$$=(-1)^{J_f-M_f}\begin{pmatrix} J_f & \lambda & J_i \\ -M_f & \mu & M_i \end{pmatrix}\langle f\|j_\lambda(qr)\|i\rangle. \quad (4)$$

In Eq. (4), J_f is the spin of the excited nuclear state and we use the notation of Edmonds[13] for the 3-j symbol.

One of the quantities we wish to determine from the cross section for inelastic scattering is the width for radiative decay of the excited state. This radiative width is given by[14]

$$\Gamma_{E\lambda}=\frac{1}{2J_f+1}\frac{8\pi(\lambda+1)\alpha}{\lambda[(2\lambda+1)!!]^2}E^{2\lambda+1}|\langle f\|r^\lambda\|i\rangle|^2, \quad (5)$$

where E is the excitation energy of the state, and the reduced matrix element is defined by

$$\int r^\lambda Y_\lambda^\mu(\hat{r})\rho_N(\mathbf{r})_{fi}d^3\mathbf{r}$$

$$=(-1)^{J_f-M_f}\begin{pmatrix} J_f & \lambda & J_i \\ -M_f & \mu & M_i \end{pmatrix}\langle f\|r^\lambda\|i\rangle. \quad (6)$$

To relate the inelastic cross section to the width for radiative decay, we use the small argument expansion for the spherical Bessel function in Eq. (4) to obtain

$$\langle f\|j_\lambda(qr)\|i\rangle=\frac{q^\lambda}{(2\lambda+1)!!}\left\{\langle f\|r^\lambda\|i\rangle - \frac{q^2}{2(2\lambda+3)}\langle f\|r^{\lambda+2}\|i\rangle+\cdots\right\}. \quad (7)$$

Equation (7) shows that the width for radiative decay is directly related to the inelastic cross section for small values of the momentum transfer q.

One method of obtaining the radiative width is to measure the inelastic cross section for small values of q and use Eq. (7) to obtain the reduced matrix element $\langle f\|r^\lambda\|i\rangle$. In practice this is difficult since the *elastic* electron-scattering cross section increases rapidly with decreasing q. The radiative tail from the elastic cross section tends to obscure the inelastic scattering.

Another method of obtaining the radiative width is to assume some model for the transition charge distribution and use this to calculate the q dependence of the inelastic form factor. This form factor is then used to extrapolate the experimental results to small values of q.

[11] See, for example, R. Hofstadter, Rev. Mod. Phys. **28**, 214 (1956).

[12] T. A. Griffy, D. S. Onley, J. T. Reynolds, and L. C. Biedenharn, Phys. Rev. **128**, 833 (1962).

[13] A. R. Edmonds, *Angular Momentum in Quantum Mechanics* (Princeton University Press, Princeton, New Jersey, 1957).

[14] J. M. Blatt and V. F. Weisskopf, *Theoretical Nuclear Physics* (John Wiley & Sons, Inc., New York, 1952).

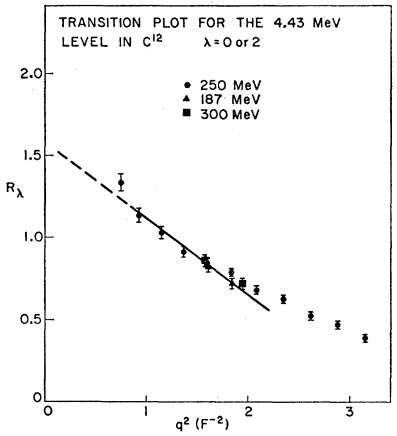

FIG. 3. Transition plot for excitation of the 4.43-MeV level in C^{12}. The ratio R_λ defined in Eq. (16) is plotted for $\lambda=0$ or 2. One cannot distinguish between these two assignments because of the ambiguity discussed in the text. The straight line shown is a least-squares fit to the seven lowest points.

A new method for extrapolating the inelastic cross section, which uses the form factor for elastic scattering and is model-independent, has been employed in this experiment. The method is similar to that proposed by Schiff[15] for electric monopole transitions.

The cross section for elastic electron scattering is written in the form

$$d\sigma/d\Omega=\sigma_{\mathrm{Mott}}Z^2|F(q^2)|^2, \tag{8}$$

with the elastic form factor defined in terms of the ground-state charge distribution by

$$F(q^2)=\int_0^\infty \rho(r)j_0(qr)r^2dr. \tag{9}$$

For small values of q, $F(q^2)$ may be written as

$$F(q^2)=1-(q^2/6)\langle r^2\rangle+(q^4/120)\langle r^4\rangle+\cdots, \tag{10}$$

where the moments of the charge distribution are defined by

$$\langle r^n\rangle=\int_0^\infty r^n\rho(r)r^2dr. \tag{11}$$

We may combine Eqs. (3), (7), and (10) to obtain

$$\lim_{q^2\to 0}\frac{F_\lambda(q^2)}{1-F(q^2)}=A_\lambda q^{\lambda-2}(1-B_\lambda q^2+\cdots), \tag{12}$$

where

$$A_\lambda=\left[\frac{4\pi}{(2J_i+1)}\right]^{1/2}\frac{6\langle f\|r^\lambda\|i\rangle}{(2\lambda+1)!!\langle r^2\rangle^\lambda}, \tag{13}$$

and

$$B_\lambda=\frac{1}{2(2\lambda+3)}\frac{\langle f\|r^{\lambda+2}\|i\rangle}{\langle f\|r^\lambda\|i\rangle}-\frac{1}{20}\frac{\langle r^4\rangle}{\langle r^2\rangle}. \tag{14}$$

[15] L. I. Schiff, Phys. Rev. **98**, 1281 (1955).

The results given in Eqs. (12), (13), and (14) cannot be used without modification for $E0$ transitions. As pointed out by Schiff,[1] the inelastic form factor for an $E0$ transition, due to the orthogonality of the initial and final nuclear wave function, has the same q dependence (for small values of q^2) as the form factor for an $E2$ transition. It follows from Eq. (12) that the appropriate extrapolation formula in the case of $E0$ transition is

$$F_0(q^2)/[1-F(q^2)]=A_0(1-B_0q^2+\cdots). \tag{15}$$

It is convenient to define the ratio R_λ as

$$\begin{aligned}R_\lambda&=F_\lambda(q^2)/q^{\lambda-2}[1-F(q^2)], \quad \lambda\neq 0\\ &=F_0(q^2)/[1-F(q^2)], \quad \lambda=0,\end{aligned} \tag{16}$$

so that in the limit of small values of q^2

$$R_\lambda=A_\lambda(1-B_\lambda q^2). \tag{17}$$

Thus if the quantity R_λ is plotted versus q^2, a straight line will be obtained for small values of q^2. This provides a possible method of obtaining the multipolarity of the observed electron-scattering transition. Only if the correct value of λ is chosen will the plot of R_λ as a function of q^2 yield a straight line at small q^2. The anomalous behavior of the $E0$ transitions discussed above prohibits using this method to distinguish $E0$ and $E2$ transitions. Once the straight-line plot is obtained, the radiative width is given in terms of the intercept, A_λ, at $q^2=0$ by the equation

$$\Gamma_{E\lambda}=\frac{(\lambda+1)}{18\lambda}\frac{2J_i+1}{2J_f+1}\alpha\langle r^2\rangle^2E^{2\lambda+1}A_\lambda^2. \tag{18}$$

Equation (18) follows directly from Eqs. (5) and (13).

For $E0$ transitions, the transition matrix element M, from which the width for pair emission can be deter-

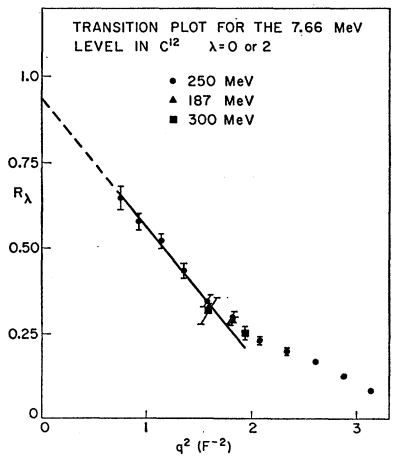

FIG. 4. Transition plot for excitation of the 7.76-MeV level in C^{12}. The ratio R_λ defined in Eq. (16) is plotted for $\lambda=0$ or 2. One cannot distinguish between these two assignments because of the ambiguity discussed in the text. The straight line shown is a least-squares fit to the seven lowest points.

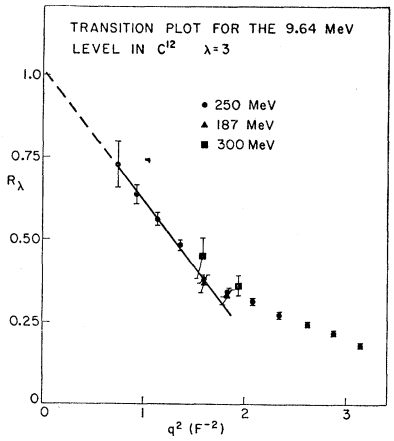

FIG. 5. Transition plot for excitation of the 9.64-MeV level in C^{12}. The ratio R_λ defined in Eq. (16) is plotted for $\lambda=3$. The straight line shown is a least-squares fit to the seven lowest points.

mined,[16] is given in terms of the intercept A_0 by

$$M=A_0\langle r^2\rangle. \tag{19}$$

Figures 3, 4, and 5, show the straight-line plots for the transitions measured in this experiment. In each case the appropriate ratio is quite well described by a straight line for small values of q^2. The straight line was obtained by applying the least-squares method to the seven lowest momentum-transfer data points. In each case the intercept of the extrapolated straight line was the same, within the statistical uncertainty, whether 5, 6, or 7 points were used in determining the straight line. The radiative widths for each of the transitions are given in Table II. The rms value of the radius was determined by a fit of the elastic-scattering data to the harmonic-well model,[11] and was found to be 2.43±0.02 F. The values of the intercepts were determined as explained above. The estimation of the uncertainties in the radiative widths include a 5% effect because of the uncertainty in the absolute cross sections.

TABLE II. Measured transition widths for excited states in C^{12}.

Level energy in MeV	λ	A_λ	Γ in eV
4.43	2	1.638±0.066	$(11.2\pm1.2)\times10^{-3}$
7.66	0	0.936±0.048	$(6.5\pm0.7)\times10^{-5}$
9.64	3	1.014±0.054	$(3.6\pm0.4)\times10^{-4}$

The radiative width for the 4.43-MeV level given in Table II compares favorably with the value of $(10.5\pm2.0)\times10^{-3}$ eV obtained by Rasmussen *et al.*[17] using resonance fluorescence methods. The value for the width of the 7.65-MeV level is within the range of $(5.5\pm3)\times10^{-5}$ eV given by Fregeau.[18]

CONCLUSIONS

The method of extrapolation presented here has the advantage that only experimentally determined quantities, namely the elastic and inelastic form factors, are used in the extrapolation. In particular, one does not use a model for the transition charge distribution to perform the extrapolation. The procedure given here applies only to the longitudinal part of the interaction so that one is restricted to scattering angles small enough that the transverse part can be neglected. It is rather difficult to set precise limits on the range of validity of the procedure. However, an estimate of the terms of order q^4 which are neglected indicates that one should obtain a straight line for values of q^2 such that $q^2\langle r^2\rangle<10$. The validity of the extrapolation can always be investigated by performing the experiments at smaller values of q^2 to see if the same straight line is obtained.

ACKNOWLEDGMENTS

We wish to thank Professor Robert Hofstadter and Professor Mason Yearion for many helpful discussions, and Mrs. C. Crannell for assistance in obtaining the data.

[16] J. R. Oppenheimer and J. S. Schwinger, Phys. Rev. **56**, 1066 (1939).

[17] V. K. Rasmussen, F. R. Metzger, and C. P. Swann, Phys. Rev. **110**, 154 (1958).

[18] J. H. Fregeau, Phys. Rev. **104**, 225 (1956).